

Received Date : 05-Feb-2016  
Revised Date : 21-May-2016  
Accepted Date : 24-May-2016  
Article type : Original Article

## **An Innovative Approach to Meteorite Analysis by Laser-Induced Breakdown Spectroscopy (LIBS)**

Giorgio S. Senesi (1)\*, Gioacchino Tempesta (2), Paola Manzari (3) and Giovanna Agrosi (2)

(1) CNR, Istituto di Nanotecnologia (NANOTEC) – PLASMI Lab, Via Amendola 122/D, 70126 Bari, Italy

(2) Dipartimento di Scienze della Terra e Geoambientali (DiSTeGeo), University of Bari, Via E. Orabona 4, 70125 Bari, Italy

(3) Istituto Nazionale di Astrofisica – Istituto di Astrofisica e Planetologia Spaziali (INAF-IAPS), via Fosso del Cavaliere 100, Roma, Italy

\*Corresponding author. e-mail: giorgio.senesi@nanotec.cnr.it

An innovative approach of double pulse laser-induced breakdown spectroscopy (DP-LIBS) coupled with optical microscopy was applied to the characterisation and quantitative analysis of the *Agoudal* iron meteorite in bulk sample and in petrographic thin section. Qualitative analysis identified the elements Ca, Co, Fe, Ga, Li and Ni in the thin section and the whole

meteorite. Two different methods, calibration-free LIBS and one-point calibration LIBS, This article has been accepted for publication and undergone full peer review but has not been through the copyediting, typesetting, pagination and proofreading process, which may lead to differences between this version and the Version of Record. Please cite this article as doi: 10.1111/ggr.12126

This article is protected by copyright. All rights reserved.

were used as complementary methodologies for quantitative LIBS analysis. The elemental composition data obtained by LIBS were in good agreement with the compositional analyses obtained by traditional methods generally applied for the analysis of meteorites, such as ICP-MS and EDS-SEM. Besides the recognised advantages of LIBS over traditional techniques, including versatility, minimal destructivity, lack of waste production, low operating costs, rapidity of analysis, availability of transportable or portable systems, etc., additional advantages of this technique in the analysis of meteorites are precision and accuracy, sensitivity to low atomic number elements such as Li and the capacity to detect and quantify Co contents that cannot be obtained by EDS-SEM.

Keywords: laser-induced breakdown spectroscopy, laser ablation, iron meteorite, chemical analysis, thin section.

Planning for future planetary missions and the rover missions, e.g., Exomars 2018, has intensified the development of innovative non-invasive or semi-invasive diagnostic analytical methods to study meteorites and planetary-analogue rock samples on the earth. In particular, there has been intense research activity over the past two decades to develop, advance and implement laser-induced breakdown spectroscopy (LIBS), as a viable and efficient analytical technique that can be applied to the study of air, water, and solid materials (Hahn and Omenetto 2012), including geological materials (Harmon *et al.* 2013, Hark and Harmon 2014, Qiao *et al.* 2014, Agrosi *et al.* 2014, Senesi 2014, Tempesta and Agrosi 2016).

Thompson *et al.* (2006) first applied a stand-off LIBS system to the analysis and fast classification of two Martian basaltic shergottite meteorites of slightly different composition, texture and grain-size. Successively, a number of meteorite samples of different groups, i.e.,

one Martian, one Lunar, three irons and one stone, were analysed qualitatively and quantitatively by Calibration Free (CF)-LIBS and classified (De Giacomo *et al.* 2007, Dell'Aglio *et al.* 2010). Motto-Ros *et al.* (2008) used an Artificial Neural Network (ANN) algorithm as the processing method for the automated quantitative LIBS analysis of a meteorite impact glass, sandstone and volcanic glass analogue of the Martian surface material collected from a meteorite impact site in Egypt. The Partial Independent Component Analysis (PICA) and Partial Least Square (PLS) methods were used to evaluate the proportion of different mineral phases and identify the distribution of mineral grain sizes in the DAG 476 Martian picritic shergottite meteorite found in the Sahara Desert of Libya (Cousin *et al.* 2012). More recently, fragments of the *Košice* meteorite were analysed by time-resolved broadband LIBS utilising the CF method to determine the mass fractions of Al, Ca, Cr, Fe, Mg, Mn, Na, Ni and Si in its crust and inner part (Hornackova *et al.* 2014). A further study (Ozdin *et al.* 2015) identified this meteorite as a monomict breccia of the petrological type H5, thus suggesting that the *Košice* chondrite probably originates from the same parent body of the H5 chondrite *Morávka* from the Czech Republic.

Studies have also begun to analyse iron meteorites, another important type of meteorite. These meteorites are genetically grouped into twelve main classes. Each group considered to be derived from a separate parent body, on the basis of distinct structural and compositional properties of magmatic iron from the crystallisation from metal melt that were products of impact and partial melting and impact events early in Earth history (Chabot *et al.* 2007). Numerous ungrouped and grouplets of iron meteorites also exist with distinct compositional characteristics, which could suggest derivation from as many as 90–100 different parent bodies.

The objective of this study was to evaluate the potential of the double pulse (DP)-LIBS technique coupled with optical microscopy to the analysis of iron meteorites. The CF-LIBS method and its recent evolution, the One-Point Calibration (OPC) method were used for the comparative quantitative analysis and characterisation in atmospheric air of a fragment of an iron meteorite, both in bulk and in petrographic thin section. The results of LIBS quantitative analysis were also compared to data obtained by traditional analytical methods, such as ICP-MS and EDS-SEM.

### **Instrumentation, principles and procedures of the LIBS technique**

A Nd-doped yttrium/aluminium garnet (Nd:YAG) pulsed laser, operating at the fundamental wavelength of 1064 nm, is preferred in most LIBS applications due to its reliable, compact and highly focused power density. A lens is used to focus the laser energy onto the sample, placed at a few centimetres to a metre distant, from the laser source. The laser blast and excites the sample surface by one or more ns-wide laser pulses of energy in the range from 1 to 150 mJ and each lasting about 5 to 20 ns. The resultant material ablation removes an amount of sample that varies from hundreds of nanograms to micrograms. During this process, a wide variety of phenomena that include rapid local heating, melting, and intense evaporation occur, which result in an overall electrically neutral plasma, consisting of a local assembly of molecular fragments, atoms, ions, and free electrons. When the elementary processes occurring between these species are locally balanced, the temperature of the plasma is considered to be in a Local Thermodynamic Equilibrium (LTE) state (Van der Mullen 1990, Hahn and Omenetto 2010). As the plasma decays or cools (a few  $\mu$ sec after the laser pulse), excited atoms in the plasma emit light of characteristic wavelengths, which is focused by a lens into a fibre-optic system that carries it to a spectrometer. The individual peaks present in the spectrum are diagnostic of the elements present in the sample and feature three

main parameters, i.e., wavelength, intensity, and shape, all of which depend on the type, amount, and surrounding of the emitting elements. The final objective of LIBS analysis is to obtain an optically thin plasma in the LTE state whose elemental composition is equivalent to that in the sample, i.e., the assumption of stoichiometric ablation that is the basis for the CF-LIBS. In this condition, the spectral line intensities will be directly related to the actual element mass fractions in the sample (Cremers and Radziemski 2006).

### **Methodologies supporting LIBS quantitative analysis**

The CF-LIBS approach is based on a plasma physics model and aims to obtain the quantitative evaluation of elements in a sample by solving sample matrix effects, i.e., reducing the quantitative statistical uncertainty, thus avoiding the cumbersome use of calibration materials and the generation of calibration curves (Ciucci *et al.* 1999, Cremers and Radziemski 2006). The CF-LIBS model is based on the assumptions that: (i) the plasma is optically thin, despite the well known LIBS self-absorption complications, and its chemical composition is the same as that of the sample; (ii) the LTE state exists in the plasma; and (iii) the plasma temperature described by the LTE model can be accurately extracted from the spectrum (Cremers and Radziemski 2006). The integrated emission intensity can, therefore, be calculated assuming the existence of a Boltzmann distribution at the LTE temperature. Furthermore, the plasma parameters can be obtained by the Saha–Boltzmann plot methodology (such as the electron temperature excitation,  $T_e$ ) from each emission line considered, while the electron density,  $N_e$ , can be calculated from the average of the Stark broadening values obtained from the different emission lines or from the Stark broadening of  $H\alpha$  emission line usually present for LIBS analysis in air. Theoretically, the CF algorithm facilitates calculation of the mass fraction of all elements present in the sample down to the detection limit of the method.

The OPC-LIBS approach, recently introduced by Cavalcanti *et al.* (2013) is a novel procedure that is a variation of the CF-LIBS method, which improves the reliability and precision of LIBS quantitative analysis. The method is simple and as fast as the usual CF-LIBS approach, and maintains the CF method advantage of being independent of matrix effects. However, the method is not completely free of reference materials, as it requires the use of one RM of known composition and a matrix matched to that of the samples to be analysed. The OPC-LIBS method permits empirical determination of the best values of crucial procedural and spectroscopic parameters that are particularly difficult to be measured experimentally, including knowledge of the response curve of the spectrometer in the spectral regions of higher interest to the LIBS analysis and of the spectral  $A_{ki}$  parameters. In particular, the intensity of a spectral line depends on the atomic population of the initial energy level and on the intrinsic probability of transition to the final energy level, which is important to reproduce exactly the nominal composition of the reference material used. The transition probability between the two energy levels for species is provided by the  $A_{ki}$  parameters whose knowledge is often imprecise or lacking. Thus, the new function ( $P(\lambda)$ ) obtained by OPC replaces the  $F(\lambda)g_iA_{ki}$  parameter from the Boltzmann equation used in the CF-LIBS method, and permits calculation of the amount of a species related to specific emission line intensities in the plasma. The function resolved by the OPC method therefore allows determination of the values used in the classical CF-LIBS analysis for the unknown samples (Cavalcanti *et al.* 2013). Overall, the method performs robustly and can improve markedly the precision of LIBS analysis with respect to the traditional CF approach, even when the composition of the samples is quite different from that of the known reference material used for the OPC approach, provided that the same spectral lines are used for the analysis of both the reference material and the unknown samples.

## Materials and methods

### Materials

The subject of this study is a fragment of a recent iron meteorite named “*Agoudal*”, from nearby the village in the High Atlas Mountains in Morocco where it was discovered (Chennaoui Aoudjehane *et al.* 2013, Meteoritical Bulletin Database 2014). Literature data report that this meteorite consists of abundant coarse-grained kamacite ( $\alpha$ -Fe, Ni), where Fe:Ni is between 90:10 to 95:5, and schreibersite (Fe, Ni)<sub>3</sub>P, rhabdite (tetragonal schreibersite) and troilite ((Fe<sub>1-x</sub>)S) (Chennaoui Aoudjehane *et al.* 2013, Schmieder *et al.* 2015). Previous ICP-MS analyses ascertained its composition to be: 5.5% *m/m* Ni and 4.1 mg g<sup>-1</sup> Co, 58  $\mu$ g g<sup>-1</sup> Ga, Ir < 0.04  $\mu$ g g<sup>-1</sup> and Au ~ 1  $\mu$ g g<sup>-1</sup> in trace quantities. Based on the aforementioned data, Chennaoui Aoudjehane *et al.* (2013) established that this meteorite belongs to the IIAB magmatic iron group. In this study, a chemical quantitative analysis was performed by LIBS on both the whole meteorite fragment and a petrographic thin section cut from it, whereas the morphological and chemical analyses were obtained by SEM-EDS on the thin section only.

Another whole bulk iron meteorite named *Dronino* was used to validate the analytical results. The *Dronino* meteorite was discovered by Oleg Guskov nearby the village of Dronino in the Ryazan oblast in Russia and belongs to the ungrouped iron meteorites. It is a fine-grained ataxite containing mainly kamacite ( $7.0 \pm 0.5\%$  *m/m* Ni and  $0.75\%$  *m/m* Co) and also taenite ( $26.3 \pm 0.5\%$  *m/m* Ni and  $0.35\%$  *m/m* Co) with sulfide inclusions (~ 10% *v/v*) (Grokhovsky *et al.* 2005).

## The LIBS experiment

A Nd:YAG Q-Switched LIBS system (Modi by Marwan Technologies) generating two laser beams in collinear geometry, both at a laser wavelength of 1064 nm (IR), was used for the acquisition of double-pulse (DP) spectra. The DP mode, which consists of two successive laser pulses that are temporally spaced by a few ns or  $\mu$ s, was adopted to better couple the laser energy to the ablated target material, thus leading to a more efficient generation of excited state atoms in the plasma and improving the LIBS signal level (Cremers *et al.* 1984). In the simplest collinear DP configuration used here (Figure 1), the two laser beams have the same propagation pathway with the second pulse reheating the plasma and increasing the amount of ablated material thus increasing its volume and emission. The LIBS system was coupled to a petrographic optical microscope using an objective lens (10X NA 0.25 WD 14.75 mm).

The LIBS analysis of the meteorite petrographic thin section (Figure 2b) was performed using three different laser energy values, i.e., 75, 100 and 120 mJ, and laser firing from one to five consecutive shots on five points aligned along three parallel directions on the surface of the thin section (Figure 2c). A maximum repetition rate of 10 Hz was used, with a delay of 1  $\mu$ s fixed between the two laser pulses. The LIBS spectra were acquired with a delay of 2  $\mu$ s after the second pulse, integrated for 2 ms, and then averaged. The plasma emission was collected using an optical fibre and the detection was performed by a double spectrometer (AvaSpec dual-channel fibre optic spectrometer by Avantes), which covered simultaneously the spectral ranges 190–400 nm (with a resolution of 0.2 nm) and 400–900 nm (with a 0.4 nm resolution).



The LIBS analysis of the rough, uncut surface of the whole *Agoudal* meteorite sample (Figure 2a) was performed inside the internal experimental chamber of the instrument using an energy of 120 mJ and a delay of 1  $\mu$ s between the two pulses. The LIBS spectra were acquired with a delay of 2  $\mu$ s after the second pulse and were integrated for 1ms. A single spectrum was acquired for each of five different points on the sample.

After acquisition and storage, the LIBS spectra were qualitatively and quantitatively analysed using two different methods, the CF-LIBS method implemented by a proprietary software (LIBS++ by Marwan Technologies), and its recent evolution, i.e., the OPC-LIBS method (Cavalcanti *et al.* 2013). The reference measurement standard for OPC was obtained from ICP-MS analyses performed by Chennaoui Aoudjehane *et al.* (2013).

#### Scanning electron microscopy

The petrographic thin section of the *Agoudal* meteorite was studied morphologically and chemically by Scanning Electron Microscopy (SEM) using a Zeiss LEO EVO50XVP coupled with an Oxford X-Max (80 mm<sup>2</sup>) silicon drift detector (SDD). Quantitative results were obtained in the secondary electron mode using an accelerating potential of 15 kV, a probe current of 500 pA, an average count rate on the whole spectrum of about 25000 output cps, a counting time of 50 s, and a working distance (WD) of 8.5 mm. The X-ray intensities were converted to elemental mass fraction in % *m/m* by the XPP correction method of Pouchou and Pichoir (1988, 1991). The accuracy of analytical data was also checked using several mineral reference materials manufactured by Micro-Analysis Consultants Ltd. In order to avoid the subjective selection of suitable analytical points, twenty points were analysed across the thin section, and then compared with the CF-LIBS and OPC-LIBS results of the whole *Agoudal* meteorite.

## Results and discussion

The versatility, potentiality, and low destructivity of the LIBS analysis of the petrographic thin section of the *Agoudal* meteorite were demonstrated by using three increasing laser energy values and an increasing number of laser shots for each energy. This procedure allowed choice of the best ratio of intensity vs. signal emission, i.e., the best emission spectra for the identification and quantification of all the elements present in the sample, and to obtain the lowest destruction of the sample.

The SEM image in Figure 3 visually displays the damage caused by the removal of sample material from the thin section due to the effect of the number of laser shots at the three energy values. The diameter and depth of each crater formed on the surface of the thin section were measured and then quantitatively plotted (Figure 4). The final crater depth obtained after five consecutive laser shots at an energy of 120 mJ was about 80  $\mu\text{m}$ , with about 15  $\mu\text{m}$  per shot, the final crater diameter was 57  $\mu\text{m}$  (Figure 4). Therefore, the energy value of 120 mJ appeared to be the best compromise between an optimal spectral emission intensity and limited sample damage. These results are, however, strictly dependent on the type of sample analysed and on the so-called “physical” matrix effects, i.e., the effects of the physical properties, like grain size, texture, reflectivity and hardness, of the sample surface on ablation parameters. These effects may cause a modification of the amount of ablated mass, thus causing a variation of the line emission intensity even if the element mass fraction is the same in the various samples. For example, sample surface roughness has been shown to affect markedly the magnitude of laser energy coupling with the surface and, as a consequence, the corresponding intensity of the LIBS signal generated (Rauschenbach *et al.* 2008).

The DP-LIBS spectra of the whole *Agoudal* meteorite sample, and of its petrographic thin section, show that the fragment studied in this work consists mainly of kamacite (Fe-Ni). In the spectral window 3100–3780 Å (Figures 5a and b) the emission lines of the elements Fe, Ni and Co can be identified. The spectra acquired on the external regions of the whole meteorite (Figure 5a) featured the emission line of Cu (Cu I at 3247 Å), which was not found in the thin section spectra (Figure 5b), and might be ascribed to a secondary alteration process. The presence of Cu can be ascribed to a miscibility gap that often occurs between taenite ( $\gamma$ -(Ni, Fe) and two other metal phases, i.e., kamacite and tetrataenite (tetragonal taenite), where  $\text{Fe} + \text{Co} \leftrightarrow \text{Ni} + \text{Cu}$  substitutions may occur (Ozdin *et al.* 2015). The additional elements detected by LIBS only in the external regions of the whole meteorite in the wavelength range 6310–6750 Å (Figure 5c), i.e., Ca (6439 and 6471 Å), Ga (6334 Å), and Li (6707 Å) might also be ascribed to alteration processes. Moreover, the presence of Li, which was detected only on the red-brown superficial alteration layer of the meteorite, would suggest an indigenous origin (Shaw *et al.* 1998).

To verify that the LTE condition is fulfilled, the excitation temperatures ( $T_{\text{ex}}$ ) and electron densities ( $N_e$ ), of the plasma were controlled after spectra acquisition and before performing the quantitative measurements. The  $T_{\text{ex}}$  value obtained by the Fe Boltzmann plot of all spots analysed ranged between 7000 K for the whole meteorite and 7550 K for the petrographic thin section. The  $N_e$  values obtained by the Stark broadening of the hydrogen line were  $3.8 \times 10^{16} \text{ cm}^{-3}$  for the whole meteorite and  $3.1 \times 10^{17} \text{ cm}^{-3}$  for the thin section. These results confirm that the LTE condition is fulfilled ( $T_{\text{ex}} > 5000 \text{ K}$ ,  $N_e > 10^{16} \text{ cm}^{-3}$ ) for each sample examined, and that the plasma conditions of all samples are comparable among each other with  $T_{\text{ex}}$  and  $N_e$  values having an experimental uncertainty of 10–15%. Some slightly higher deviations may be due to small differences in the ablation efficiency and/or to the different dimensions of grains/minerals.

Quantitative analysis of the *Agoudal* meteorite was performed using both CF-LIBS and OPC-LIBS methods. Table 1 presents the compositional results obtained by LIBS analysis of both the petrographic thin section and the bulk meteorite in comparison with the corresponding results from EDS-SEM analysis, and the reference ICP-MS data from Chennaoui Aoudjehane *et al.* (2013). There is a good agreement amongst all methods. The small differences between LIBS and ICP-MS data may be ascribed to the much greater amount of sample (about 1 g) that is analysed by ICP-MS, thus reducing markedly the matrix effects with respect to LIBS. However, LIBS results from heterogeneous samples may differ significantly from those obtained by conventional bulk analysis techniques, such as ICP-MS. This is because LIBS is a point analysis technique that can analyse only a portion of the sample of the dimension of the focused laser spot, i.e., the ablated mass is less than a microgram for each laser shot. However, the average elemental composition, which is more representative of the whole meteorite, can be obtained by translating the sample during LIBS analysis in order to ablate different points. This procedure improves the analytical results from the statistical point of view, and thus allows a meaningful comparison of LIBS to other bulk techniques often employed in meteorite analysis.

To validate the OPC method, the ungrouped iron meteorite *Dronino*, consisting mainly of kamacite (Grokhovsky *et al.* 2005), was analysed by LIBS. The OPC quantitative data were obtained using the *Agoudal* meteorite as the calibration material and are shown in Table 1. A good agreement is found by comparing our data with the *Dronino* literature data, which confirms the validity of the OPC method.

The EDS-SEM spectrum acquired for the thin section of the *Agoudal* meteorite (Figure 6) shows that the Co present in this meteorite cannot be detected and quantified by this technique because the resolution limit of the SDD (125 eV on Mn K $\alpha$ ) is not sufficient to distinguish the Fe K $\beta$  line from the Co K $\alpha$  line. By contrast, the Co emission lines in the LIBS spectrum are well recognisable, thus confirming the added value of this technique.

## Conclusions

The innovative approach of this work consists of using the LIBS technique coupled with a petrographic microscope, which allows the chemical analysis to be performed directly on a meteorite thin section in a unique experiment without the use of reference materials and without using a controlled atmosphere. The supporting analytical methods used in this work, i.e., CF-LIBS and OPC-LIBS, can provide the elemental and chemical composition of the meteorite with acceptable accuracy. Another advantage of the LIBS method is the small amount of sample consumed compared with the much greater amounts needed for ICP-MS analysis or other traditional analytical techniques. The compositional data obtained by LIBS are in very good agreement with those obtained by ICP-MS and EDS-SEM.

## Acknowledgements

The authors are grateful to Prof. P. Acquafredda and to N. Mongelli of the Earth and Geo-environmental Department of University of Bari (Italy) for their assistance during SEM analyses. This work was funded by National Project PONa3\_00369 “SISTEMA” of the University of Bari “A. Moro” funded by MIUR.

## References

Agrosi G., Tempesta G., Scandale E., Legnaioli S., Lorenzetti G., Pagnotta S., Palleschi V., Mangone A. and Lezzerini M. (2014)

Application of laser induced breakdown spectroscopy to the identification of emeralds from different synthetic processes. **Spectrochimica Acta Part B**, **102**, 48–51.

Cavalcanti G.H., Teixeira D.V., Legnaioli S., Lorenzetti G., Pardini L. and Palleschi V. (2013)

One-point calibration for calibration-free laser-induced breakdown spectroscopy quantitative analysis. **Spectrochimica Acta Part B**, **87**, 51–56.

Chabot N.L., Saslow S.A., McDonough W.F. and McCoy T.J. (2007)

The effect of Ni on element partitioning during iron meteorite crystallization. **Meteoritics and Planetary Science**, **42**, 1735–1750.

Chennaoui Aoudjehane H., Garvie L.A.J., Herd C.D.K., Chen G. and Aboulahris M. (2013)

Agoudal: The most recent iron meteorite from Morocco. **76th Meeting of the Meteoritical Society**, Edmonton, Canada, abstract 5026.

Ciucci A., Corsi M., Palleschi V., Rastelli S., Salvetti A. and Tognoni E. (1999)

New procedure for quantitative elemental analysis by laser-induced plasma spectroscopy. **Applied Spectroscopy**, **53**, 960–964.

**Cousin A., Sautter V., Fabre C., Maurice S. and Wiens R.C. (2012)**

Textural and modal analyses of picritic basalts with ChemCam laser-induced breakdown spectroscopy. **Journal of Geophysical Research**, **117**, E10002.

**Creers D.A., Radziemski L.J. and Loree T.R. (1984)**

Spectrochemical analysis of liquids using the laser spark. **Applied Spectroscopy**, **38**, 721–729.

**Creemers D.A. and Radziemski L.J. (2006)**

Handbook of laser-induced breakdown spectroscopy. **Wiley (Chichester)**.

**De Giacomo A., Dell'Aglio M., De Pascale O., Longo S. and Capitelli M. (2007)**

Laser induced breakdown spectroscopy on meteorites. **Spectrochimica Acta Part B**, **62**, 1606–1611.

**Dell'Aglio M., De Giacomo A., Gaudiuso R., De Pascale O., Senesi G.S. and Longo S. (2010)**

Laser induced breakdown spectroscopy applications to meteorites: Chemical analysis and composition profiles. **Geochimica et Cosmochimica Acta**, **74**, 7329–7339.

**Grokhovsky V.I., Ustyugov V.F., Badyukov D.D. and Nazarov M.A. (2005)**

Dronino: an ancient iron meteorite shower in Russia. **Lunar and Planetary Science XXXVI**, Abstract no. 1692.

**Hahn D.W. and Omenetto N. (2010)**

Laser-induced breakdown spectroscopy (LIBS), part I: Review of basic diagnostics and plasma–particle interactions: Still-challenging issues within the analytical plasma community. **Applied Spectroscopy**, **64**, 335A–366A.

**Hahn D.W. and Omenetto N. (2012)**

Laser-induced breakdown spectroscopy (LIBS), part II: Review of instrumental and methodological approaches to material analysis and applications to different fields. **Applied Spectroscopy**, **66**, 347–419.

**Hark R.R. and Harmon R.S. (2014)**

Geochemical fingerprinting using LIBS. In: **Musazzi S. and Perini U. (eds), Laser-induced breakdown spectroscopy theory and applications. Springer (Heidelberg)**, 309–344.

**Harmon R.S., Russo R.E. and Hark R.R. (2013)**

Applications of laser-induced breakdown spectroscopy for geochemical and environmental analysis: A comprehensive review. **Spectrochimica Acta Part B**, **87**, 11–26.

**Hornáčková M., Plavčan J., Rakovsky J., Porubčany V., Ozdin D. and Veis P. (2014)**

Calibration-free laser induced breakdown spectroscopy as an alternative method for found meteorite fragments analysis. **The European Physical Journal Applied Physics**, **66**, 10702.

**Meteoritical Bulletin Database (2014)**

Entry for Agoudal: <http://www.lpi.usra.edu/meteor/metbull.php?code=57354> (Date last accessed: 15 September 2013).



**Motto-Ros V., Koujelev A.S., Osinski G.R. and Dudelzak A.E. (2008)**

Quantitative multielemental laser-induced breakdown spectroscopy using artificial neural networks. **Journal of the European Optical Society - Rapid Publications**, **3**, 08011.

**Ozdin D., Plavcan J., Hornackova M., Uher P., Porubcan V., Veis P., Rakovsky J., Toth J., Konecny P. and Svoren J. (2015)**

Mineralogy, petrography, geochemistry, and classification of the Košice meteorite. **Meteoritics and Planetary Science**, **50**, 864–879.

**Pouchou J.L. and Pichoir F. (1988)**

A simplified version of the “PAP” model for matrix corrections in EPMA. **In: Newbury D.E. (ed.), Microbeam analysis. San Francisco Press**, 315–318.

**Pouchou J.L. and Pichoir F. (1991)**

Quantitative analysis of homogeneous or stratified microvolumes applying the model “PAP”. **In: Heinrich K.F.J. and Newbury D.E. (eds), Electron probe quantitation. Plenum Press (New York)**, 31–75.

**Qiao S., Ding Y., Tian D., Yao L. and Yang G. (2014)**

A review of laser-induced breakdown spectroscopy for analysis of geological materials. **Applied Spectroscopy Reviews**, **50**, 1–26.

**Rauschenbach I., Lazic V., Pavlov S.G., Hubers H.-W. and Jessberger E.K. (2008)**

Laser induced breakdown spectroscopy on soils and rocks: Influence of the sample

temperature, moisture and roughness. **Spectrochimica Acta Part B**, **63**, 1205–1215.

**Schmieder M., Chennaoui Aoudjehane H., Buchner E. and Tohver E. (2015)**

Meteorite traces on a shatter cone surface from the Agoudal impact site, Morocco. **Geological Magazine**, **152**, 751–757.

**Senesi G.S. (2014)**

Laser-induced breakdown spectroscopy (LIBS) applied to terrestrial and extraterrestrial analogue geomaterials with emphasis to minerals and rocks. **Earth Science Reviews**, **139**, 231–267.

**Shaw D.M., Higgins M.D., Truscott M.G. and Middleton T.A. (1998)**

Boron contamination in polished thin sections of meteorites: Implications for other trace-element studies by alpha-track image or iron microprobe. **American Mineralogist**, **73**, 894–900.

**Tempesta G. and Agrosi G. (2016)**

Standardless, minimally destructive chemical analysis of red beryls by means of laser induced breakdown spectroscopy. **European Journal of Mineralogy**, doi: 10.1127/ejm/2016/0028-2529 (in press).

**Thompson J.R., Wiens R.C., Barefield J.E., Vaniman D.T., Newsom H.E. and Clegg S.M. (2006)**

Remote laser induced breakdown spectroscopy analyses of Dar al Gani 476 and Zagami Martian meteorites. **Journal of Geophysical Research**, **111**, E05006.

**Van der Mullen J.A.M. (1990)**

Excitation equilibria in plasmas: A classification. **Physics Reports**, **2**, 109–120.

### **Figure captions**

Figure 1. Schematic figure of the experimental set up used for the analysis of the thin section and whole meteorite.

Figure 2. Images of (a) a fragment of the whole meteorite *Agoudal* IIAB and (b) of a thin section cut from it; (c) magnified optical image of LIBS shot area on the thin section.

Figure 3. SEM image of ablation craters obtained on the thin section of the *Agoudal* meteorite as a function of laser shot numbers and laser energy, where halos of oxidation are visible around the largest craters due to interaction between the laser and sample.

Figure 4. Crater diameters and crater depth (only at 120 mJ) in thin section of the *Agoudal* meteorite as a function of the number of shots at the three energy values used.

Figure 5. DP-LIBS spectra and peak identification (Fe, Ni, Co, Cu) in the wavelength range 3100–3780 Å of (a) the whole *Agoudal* meteorite sample and (b) of its thin section; (c) DP-LIBS spectra in the wavelength range 6310–6750 Å of the thin section (below) and whole sample (above), with the emission lines of Ca, Ga and Li.

Figure 6. EDS-SEM spectrum of the thin section of the *Agoudal* meteorite.

Table 1.

Comparison of element mass fraction data (in % *m/m*) obtained from different chemical analyses in the literature and those obtained in this study (in grey) of the whole meteorite and its thin section for the *Agoudal* and for the whole *Dronino* iron meteorites

Element	<i>Agoudal meteorite</i>						<i>Dronino meteorite</i>	
	ICP-MS*	EDS-SEM	CF-LIBS <sup>†</sup>	OPC-LIBS <sup>†</sup>	CF-LIBS <sup>§</sup>	OPC-LIBS <sup>§</sup>	EPMA <sup>DR*</sup>	OPC-LIBS <sup>§DR</sup>
Fe	94.1	94.41 ± 0.13	94.41 ± 0.31	94.10 ± 0.05	94.94 ± 0.43	94.40 ± 0.28	92.2	92.73 ± 1.64
Ni	5.5	5.57 ± 0.14	4.36 ± 0.44	5.31 ± 0.3	4.72 ± 0.43	5.47 ± 0.21	7.0 ± 0.5	6.26 ± 1.23
Co	0.41	N.D. <sup>#</sup>	1.24 ± 0.14	0.59 ± 0.25	0.58 ± 0.3	0.22 ± 0.17	0.75	1.02 ± 0.72

\*Reference data from Chennaoui Aoudjehane *et al.* (2013)

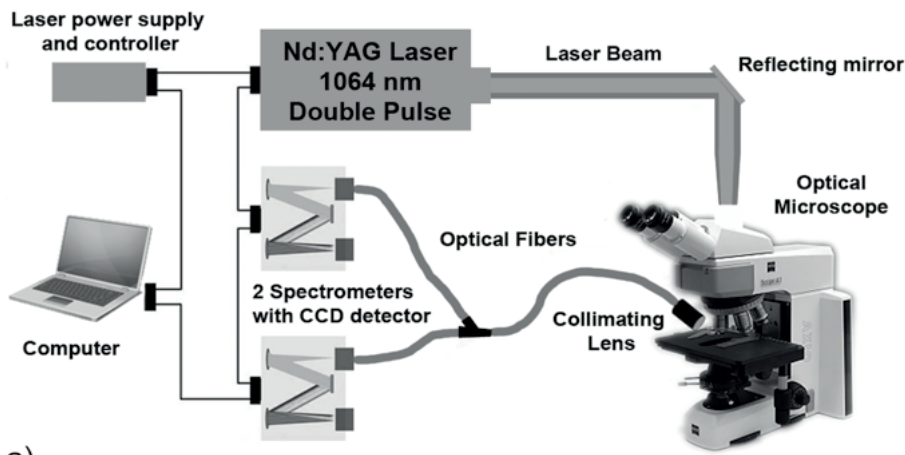
<sup>†</sup>Thin meteorite section

<sup>§</sup>Whole meteorite

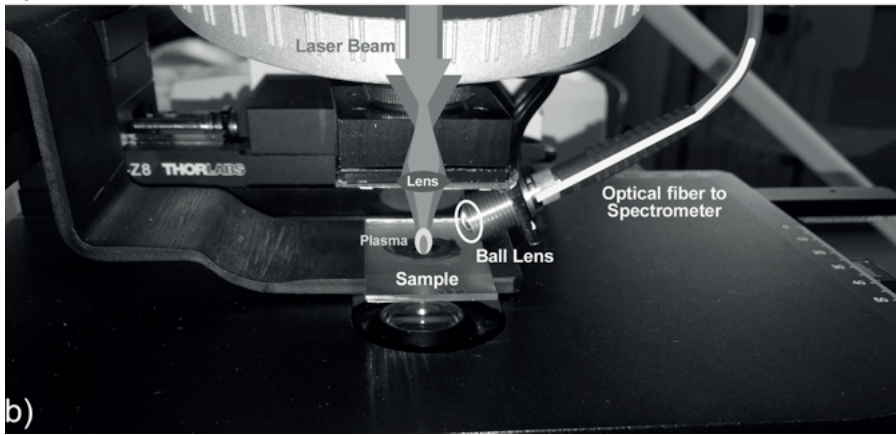
<sup>DR</sup> = Dronino

EPMA <sup>DR\*</sup> = Electron probe microanalysis reference data from Grokhovsky *et al.* (2005)

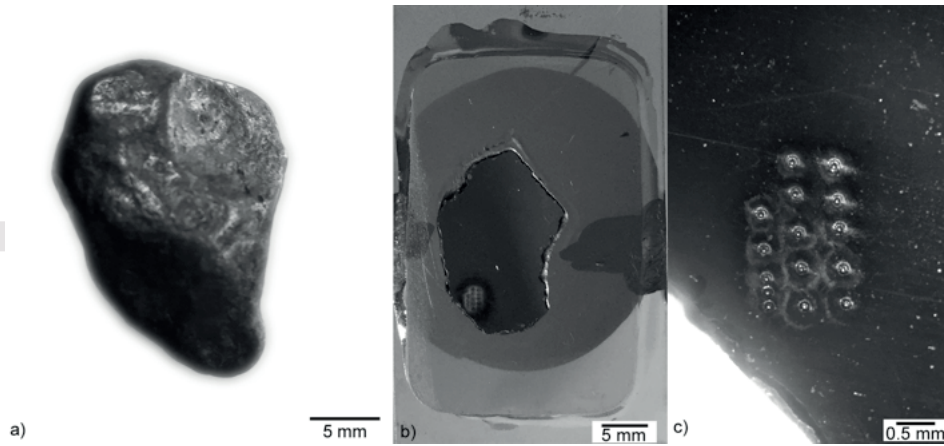
<sup>#</sup>N.D. = not determined



a)



b)



a)

5 mm

b) 5 mm

c) 0.5 mm

